

## CRYSTALLOGRAPHIC AND MAGNETIC STRUCTURE OF $Dy_3Ge_5$ AND $DyGe_{1.9}$

P. SCHOBINGER-PAPAMANTELLOS\*

*Institut für Kristallographie und Petrographie, ETHZ, CH-8092 Zürich (Switzerland)*

D. B. DE MOOIJ and K. H. J. BUSCHOW

*Philips Research Laboratories, 5600 JA Eindhoven (The Netherlands)*

(Received March 30, 1990)

### Summary

The crystal structure and the magnetic structure of the compounds  $Dy_3Ge_5$  and  $DyGe_{1.9}$  were investigated by neutron diffraction. The compound  $Dy_3Ge_5$  has an orthorhombic structure derived from the tetragonal  $\alpha$ - $ThSi_2$  structure, the ordered germanium vacancies being described by a density and displacive modulation. Below  $T_N = 12$  K  $Dy_3Ge_5$  orders antiferromagnetically but the magnetic structure is fairly complex. The compound  $DyGe_{1.9}$  has an orthorhombic structure that is quite different from  $Dy_3Ge_5$  although it can also be derived from the  $\alpha$ - $ThSi_2$  structure type.  $DyGe_{1.9}$  gives rise to a uniaxial antiferromagnetic moment arrangement below  $T_N = 29$  K.

### 1. Introduction

The composition and crystal structure of intermetallic compounds of the type  $DyGe_x$  occurring in the range  $1.6 \leq x \leq 2.0$  were investigated by Sekizawa [1] who also studied their magnetic properties. He reported the existence of three types of compounds located in a fairly narrow concentration range. The first of these compounds,  $DyGe_{1.62}$ , occurs in two modifications. The low temperature (LT) phase crystallizes in the defect  $AlB_2$  structure, the high temperature (HT) phase in the defect  $\alpha$ - $ThSi_2$  structure. The latter type of structure was also found for slightly higher germanium concentrations ( $DyGe_{1.67}$ ). At still higher germanium concentrations a compound of the composition  $DyGe_2$  occurs; this was reported by Sekizawa to have a crystal structure with orthorhombic symmetry, but no structure determination was made. This orthorhombic structure was observed by this author for germanium concentrations larger than  $DyGe_{1.85}$ . More recently the  $Dy$ - $Ge$

\*Permanent guest scientist at the Laboratorium für Neutronenstreuung, CH-5232 Villigen, PSI, Switzerland.

phase diagram was studied by Eremenko *et al.* [2]. These authors observed the  $\text{AlB}_2$  structure type for a composition  $\text{Dy}_{1.04}\text{Ge}_{1.56}$  while for  $\text{DyGe}_{1.63}$  they found the  $\alpha\text{-ThSi}_2$  structure type.

In a previous investigation [3] we showed that the germanium vacancies in the defect  $\alpha\text{-ThSi}_2$  type structure of  $\text{TbGe}_{1.67}$  ( $\text{Tb}_3\text{Ge}_5$ ) have a high degree of ordering at particular germanium positions. This ordering leads to a new type of orthorhombic unit cell containing six unit cells of the basic  $\alpha\text{-ThSi}_2$  type [3]. By X-ray diffraction this ordered defect structure can be distinguished from the  $\alpha\text{-ThSi}_2$  structure by the occurrence of weak superstructure lines, accompanying the strong main reflections of the  $\alpha\text{-ThSi}_2$  type. On the basis of the weak reflection lines found in the X-ray diagram of  $\text{Dy}_3\text{Ge}_5$ , we also proposed that the latter compound adopts the orthorhombic structure rather than the defect  $\alpha\text{-ThSi}_2$  structure [4]. In the present investigation we have studied the crystal structure of  $\text{Dy}_3\text{Ge}_5$  in more detail by using neutron diffraction.

In a previous investigation of the Tb-Ge system we reported on a novel structure type found in  $\text{TbGe}_2$  [5]. Since our X-ray data on  $\text{DyGe}_2$  led us to believe that  $\text{DyGe}_2$  is of the same structure type we have included a structure determination by means of neutron diffraction for  $\text{DyGe}_2$  in our study.

According to Sekizawa [1], the magnetic properties depend strongly on stoichiometry and crystal structure. The LT modification of  $\text{DyGe}_{1.62}$  orders anti-ferromagnetically at 23 K while the HT modification becomes ordered only at 6.5 K. The compound of composition  $\text{DyGe}_{1.67}$  of the  $\alpha\text{-ThSi}_2$  type orders at 12 K while  $\text{DyGe}_2$  orders at 28 K (see also Table 1). This prompted us to include in our neutron diffraction study magnetic structures as well as crystallographic structures.

## 2. Experimental details

Samples of composition  $\text{DyGe}_x$  with  $x = 1.67, 1.70, 1.75, 1.80, 1.85, 1.90, 1.95, 2.00$  and  $2.50$  were prepared by arc melting in an atmosphere of purified argon gas. The purity of the starting materials was 99.9% for dysprosium and 99.99% for germanium. After arc melting the samples were vacuum annealed in the temperature range 800–1000 °C for several weeks. After annealing the samples

TABLE 1

Structural and magnetic data of compounds  $\text{DyGe}_x$  reported in ref. 1. Results of the present investigation are given in parentheses

Sample	Type	$a$ (nm)	$b$ (nm)	$c$ (nm)	$T_N$ (K)
$\text{DyGe}_{1.62}$	$\text{AlB}_2$	0.3654	—	0.4146	23
$\text{DyGe}_{1.62}$	$\alpha\text{-ThSi}_2$	0.4047	—	1.3716	6.5
$\text{DyGe}_{1.67}$	$\alpha\text{-ThSi}_2$	0.4054 (0.4051)	—	1.368 (1.3678)	12 (12)
$\text{DyGe}_{2.00}$	$\text{TbGe}_2$	0.799 (0.3986)	8.12 (0.4091)	1.489 (2.98075)	28 (29)

were powdered and examined by standard X-ray diffraction using Cu K $\alpha$  radiation.

The neutron data were collected on powdered samples of nominal compositions DyGe<sub>1.67</sub> and DyGe<sub>2</sub>, with the double axis multi counter system (DMC) at the Reactor Saphir, Würenlingen, in the temperature range 2–60 K using  $\lambda = 1.7078 \text{ \AA}$ . The step increment of the diffraction angle  $2\theta$  was  $0.10^\circ$ . Both dysprosium samples were examined by neutron diffraction using a tubular vanadium sample holder of thickness 1.0 mm and outer diameter 10 mm in order to deal with the high absorption cross-section of dysprosium for neutrons. The data were corrected for absorption and evaluated by the line profile analysis method [6–8]. The scattering lengths and magnetic form factors are those of ref. 9 and ref. 10 respectively.

### 3. Experimental results

#### 3.1. X-ray data

The X-ray diffraction data obtained from DyGe<sub>1.67</sub> after annealing at 1000 °C showed the pattern due to the  $\alpha$ -ThSi<sub>2</sub> structure. It was accompanied by low intensity superstructure lines, as already mentioned in the introduction.

The X-ray data of DyGe<sub>x</sub> samples with  $x \geq 1.70$  annealed at 850 °C all have a main phase exhibiting an X-ray pattern as observed previously for TbGe<sub>2</sub>. The X-ray patterns were single phase only for the sample with  $x = 1.90$ . The samples with  $x < 1.90$  were found to contain the phase Dy<sub>3</sub>Ge<sub>5</sub>, the amount of which decreased with germanium concentration. The sample DyGe<sub>2.5</sub> showed essentially the same type of reflection lines as the sample DyGe<sub>2</sub> but there were additional lines in its X-ray diagram belonging to a phase more rich in germanium than DyGe<sub>2</sub>. A survey of the structures and the corresponding lattice constants as derived from the X-ray data is given in Table 1.

#### 3.2. Crystallographic and magnetic structure of Dy<sub>3</sub>Ge<sub>5</sub>

The neutron diffraction patterns obtained for the compound with  $x = 1.67$  in the paramagnetic state at 293 K are shown in Fig. 1. The main reflections can be described by means of the tetragonal  $\alpha$ -ThSi<sub>2</sub> type of structure. However, superstructure lines can also be recognized, indicating the orthorhombic Tb<sub>3</sub>Ge<sub>5</sub> structure. These superstructure lines are much weaker than in Tb<sub>3</sub>Ge<sub>5</sub> owing to the fact that the nuclear scattering length of dysprosium is twice that of germanium and terbium and therefore its contribution dominates the scattered intensities. Table 2 displays the refined parameters at 293 K.

Neutron data in the magnetically ordered state were obtained at 4.2 K. The data show that the magnetic ordering consists of at least two different contributions. The broad and wavy peaks concentrated in the low  $2\theta$  region in Fig. 2 indicate the predominance of short-range order effects. These short-range order effects were found to persist to the lowest temperature (1.2 K) considered in this

**Dy<sub>3</sub>Ge<sub>5</sub> 293 K**

Neutron Wavelength 1.7078 Å

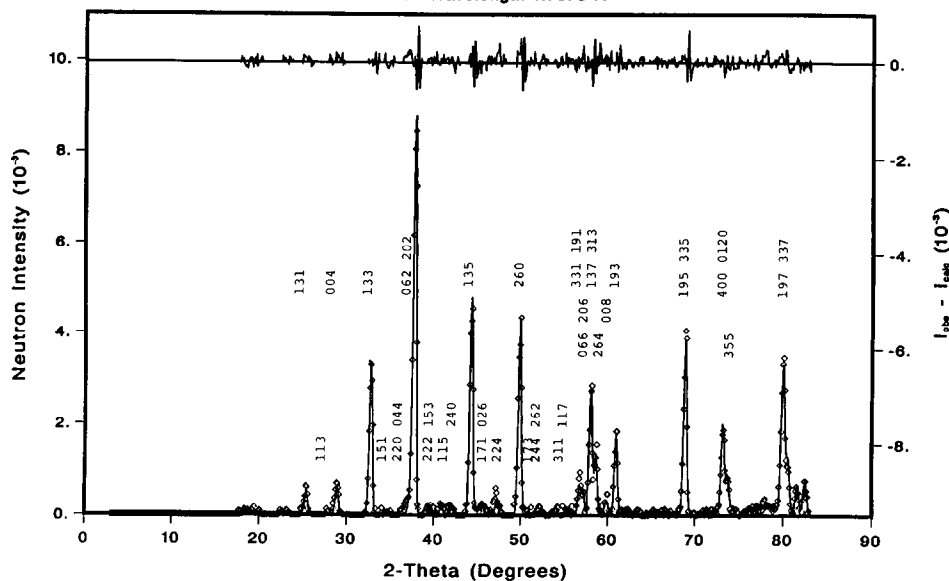


Fig. 1. Observed (data points) and calculated (solid line) neutron diffraction pattern of Dy<sub>3</sub>Ge<sub>5</sub> in the paramagnetic state at 293 K. The calculation was carried out in the orthorhombic cell (Table 2) enlarged with respect to the tetragonal  $\alpha$ -ThSi<sub>2</sub> type cell.

TABLE 2

Refined parameters derived from the 293 K neutron data in the paramagnetic state of Dy<sub>3</sub>Ge<sub>5</sub>. The overall temperature factor was kept constant owing to correlations with the absorption

Fdd2 atom	Site	Dy <sub>3</sub> Ge <sub>5</sub> 293 K		
		x	y	z
Dy(1)	8a	0	0	0 <sup>a</sup>
Dy(2)	16b	0.756(3)	0.082(1)	0.261(1)
Ge(1)	8a	0	0	0.428(2)
Ge(2)	16b	0.818(4)	0.073(1)	0.653(2)
Ge(3)	16b	0.776(5)	0.082(1)	0.827(2)
<i>a, b, c</i> (nm)		0.5729(1)	1.7190(2)	1.3678(1)
		<i>R</i> <sub>n</sub> = 9%	<i>R</i> <sub>wp</sub> = 17%	<i>R</i> <sub>exp</sub> = 7%
				$\chi^2$ = 4%

<sup>a</sup>Fixed parameter.

investigation. A large number of long-range order magnetic peaks overlap with the wavy background in the low  $2\theta$  region. A first attempt to index the pattern led to a very large magnetic cell ( $2a, 2b, c$ ) but the very poor resolution of the present data does not allow a quantitative analysis.

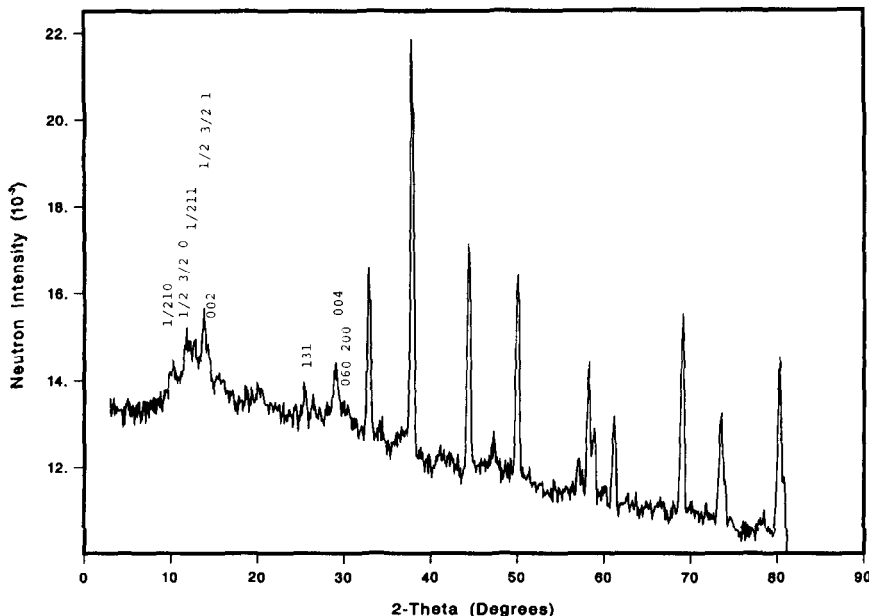
Dy<sub>3</sub>Ge<sub>5</sub>, 4.2 K, 1.7078 Å

Fig. 2. Neutron diffraction pattern observed for Dy<sub>3</sub>Ge<sub>5</sub> in the magnetically ordered state showing predominantly short-range order effects in the low  $2\theta$  region.

We may, however, state that this diffraction pattern found is more similar to the pattern for Tb<sub>3</sub>Ge<sub>4</sub>Si than to that of Tb<sub>3</sub>Ge<sub>5</sub>. The latter compound is already known [3] to have a complex canted moment arrangement ( $k=0$ ) with  $z$  as the main axis of antiferromagnetism. In Tb<sub>3</sub>Ge<sub>4</sub>Si we can observe, besides the reflections associated with  $k=0$ , a second set of reflections which indicates the presence of more than one modulation vector in the ( $x, y, 0$ ) plane and a reduction of the  $k=0$  contributions. In DyGe<sub>1.67</sub> only the superstructure contributions can be observed. The  $k=0$  contributions are zero, as can be inferred from the intensities of the 131 (nuclear) reflections at  $2\theta = 25.5^\circ$  and 200; 060 at  $2\theta = 34.6^\circ$ . In view of this complex magnetic behaviour we have the impression that a further understanding of the stoichiometric compound Dy<sub>3</sub>Ge<sub>5</sub> would need support from single-crystal data. It is possible that in Dy<sub>3</sub>Ge<sub>5</sub> a superstructure with more than one wavevector and higher harmonics exists which will be investigated in the near future. A difficulty we often encounter in systems forming superstructures is the possible coexistence of more than one modulation vector of the same basic structure.

### 3.3. Crystallographic and magnetic structure of DyGe<sub>1.9</sub>

The existence of a new type of orthorhombic structure for compounds of the type RGe<sub>2</sub> reported by us before in the Tb-Ge system has been verified in the course of the present investigation for the Dy-Ge system. This structure was

observed in the single-phase condition only for the composition  $x = 1.90$ . It has been possible to index the X-ray diagram obtained for a sample with the nominal composition  $\text{DyGe}_2$  on the basis of an orthorhombic unit cell with the lattice parameters  $a = 0.4100$  nm,  $b = 2.9753$  nm and  $c = 0.4005$  nm. Systematic extinctions led to the space group  $Cmmm$  (number 65). Using the same trial structure as found for  $\text{TbGe}_2$ , the parameter refinement converged to an  $R$  factor of 10%. Results of the refinement of the X-ray data are summarized in Table 3.

The same positional parameters were found from the refinement of the room temperature neutron data (full lines in Fig. 1). The refined parameters are listed in Table 3. It is interesting to note that the refinement of the neutron data suggests a deviation from the stoichiometric  $\text{DyGe}_2$  composition. It follows from the refinement that the 4i position of the Ge(4) atoms is only half-filled, which results in the composition  $\text{DyGe}_{1.85(5)}$ . The diffraction pattern at 293 K contains a few non-overlapping foreign lines denoted by (i) in Fig. 3 which do not belong to the dysprosium-richest compound  $\text{DyGe}_{2.85}$  reported by Eremenko *et al.* [2]. By comparing the observed X-ray pattern reported by Sekizawa [1] with the present data in Table 4, it becomes clear that not all the lines observed by Sekizawa belong to the  $\text{DyGe}_2$  pattern.

Besides the high absorption of the sample, the presence of impurity lines also has an unfavourable influence on the accuracy of the refined parameters and leads to rather high  $R$  factors. The X-ray results suggest  $\text{DyGe}_{1.9}$  as the composition of the orthorhombic compound since samples of composition  $\text{DyGe}_{1.85}$  belong to the two-phase region between  $\text{Dy}_3\text{Ge}_5$  and  $\text{DyGe}_{1.9}$ . The deviation from the 1:2 stoichiometry is closely connected with the interatomic distances in  $\text{DyGe}_{1.85}$ . The calculated values shown in Table 5 indicate that the shortest interatomic Ge-Ge distances (2.204(12)) occur for the three-coordinated Ge(4) atom. Since the Ge(4)-Ge(4) distance is even shorter than the Ge-Ge covalent bond length (2.44 Å), a partial occupation of this position would allow the system to overcome its internal frustration. The refinement of neutron data converged to  $R_n = 9\%$ ,  $R_{wp} = 17\%$ ,  $R_{exp} = 7\%$  and  $x^2 = 2.5\%$ .

The neutron diffraction pattern obtained in the magnetically ordered state on the sample of nominal composition  $\text{DyGe}_2$  is shown in Fig. 4. The pattern was indexed with the same unit cell as the nuclear structure ( $k = 0$ ). The dysprosium atoms are distributed over two special symmetry positions: Dy(1) at 4i (0y0) and Dy(2) at 4j (0y1/2). The atomic arrangement in the structure of  $\text{DyGe}_2$  entails a stacking of paired layers consisting of trigonal prisms of dysprosium atoms, the prisms being centred by germanium atoms (see Fig. 5). This kind of stacking resembles that of the  $\alpha\text{-ThSi}_2$  and  $\alpha\text{-GdSi}_2$  types of structure (shown in the bottom part of Fig. 5). The prism axes are in the (010) plane and point in the  $a$  or  $b$  directions. Between successive layers the prism axis rotates by 90°.

Besides the orthorhombic deformation a further difference with the  $\alpha\text{-ThSi}_2$  structure is that the stacking of the trigonal prisms of paired dysprosium layers is interrupted along the longest axis  $b$  by a germanium layer at the mirror plane  $m_y = (y = 0, 1/2)$ .

The refined parameters of the 4.2 K data are given in Table 3. The resulting magnetic structure corresponds to a uniaxial antiferromagnetic arrangement of the

TABLE 3  
Refined parameters from the 293 K nuclear data and 4.2 K magnetically ordered data of DyGe<sub>1.90</sub> compared with the 293 K X-ray data. The neutron refinement suggests the composition DyGe<sub>1.85(5)</sub>

C <sub>n</sub> m <sub>m</sub> atom	Site	Neutron diffraction at 293 K			Neutron diffraction at 4.2 K			X-ray diffraction at 293 K			
		x	y	z	x	y	z	$\mu_z$ (Dy) ( $\mu_B$ )	x	y	z
Dy(1)	4i	0.0	0.4247(2)	0.0	0.0	0.4245(4)	0.0	9.4(2)	0.0	0.4249	0.0
Dy(2)	4j	0.0	0.3101(2)	0.5	0.0	0.3093(4)	0.5	-8.6(2)	0.0	0.3091	0.5
Ge(1)	2a	0.0	0.0	0.0	0.0	0.0	0.0	—	0.0	0.0	0.0
Ge(2)	2c	0.5	0.0	0.5	0.5	0.0	0.5	—	0.5	0.0	0.5
Ge(3)	4i	0.0	0.1581(5)	0.0	0.0	0.1592(8)	0.0	—	0.0	0.1538	0.0
Ge(4) <sup>a</sup>	4i	0.0	0.2362(8)	0.0	0.0	0.2391(1)	0.0	—	0.0	0.2424	0.0
Ge(5)	4j	0.0	0.1049(6)	0.5	0.0	0.1047(8)	0.5	—	0.0	0.1053	0.5
<i>a, b, c</i> (nm)		0.4091(1)	2.9807(4)	0.3987(1)	0.4072(1)	2.9766(4)	0.3964(1)	<i>R</i> <sub>n</sub> = 9% <i>R</i> <sub>wp</sub> = 7% <i>R</i> <sub>exp</sub> = 7% <i>χ</i> <sup>2</sup> = 2.5%			0.4100
<i>R</i> factors		<i>R</i> <sub>n</sub> = 9% <i>R</i> <sub>wp</sub> = 17% <i>R</i> <sub>exp</sub> = 17% <i>R</i> <sub>wp</sub> = 8.8% <i>R</i> <sub>exp</sub> = 7% <i>χ</i> <sup>2</sup> = 3%			<i>R</i> <sub>n</sub> = 10%			2.9753			0.4005

<sup>a</sup>This position is only half occupied.

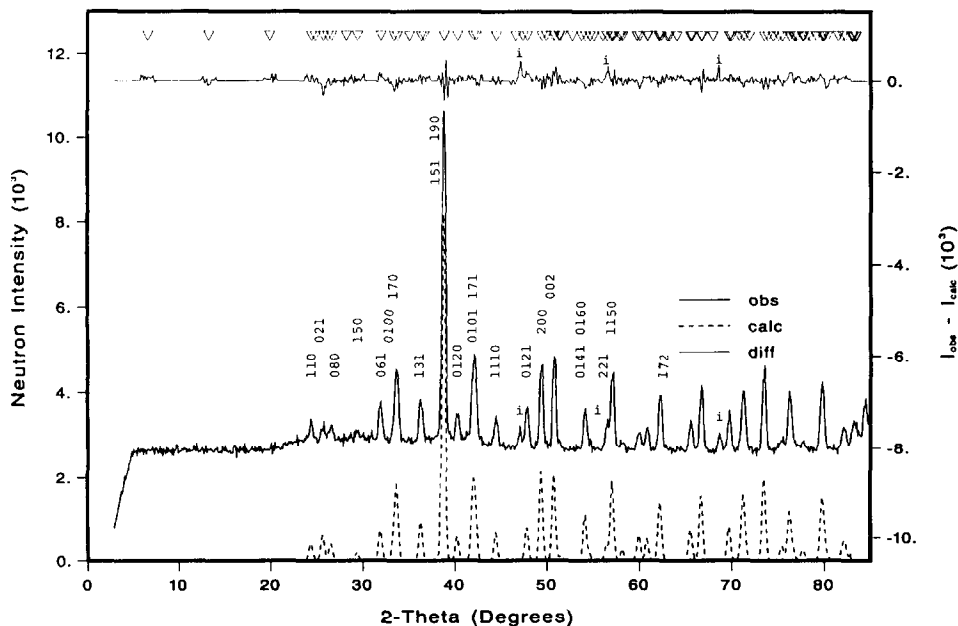
DyGe<sub>2</sub>, 293 K, 1.7078 Å

Fig. 3. Observed (solid line) and calculated (broken line) neutron diffraction pattern of DyGe<sub>2</sub> in the paramagnetic state at 293 K. The indexing refers to the X-ray lines reported in ref. 1 and (i) refers to an unknown impurity phase.

moments of the two types of dysprosium position, with the dysprosium moments pointing into the *c* direction. This stacking can be seen as an alternating  $+-+ - \dots$  stacking of ferromagnetic dysprosium layers along the longest orthorhombic axis *b*. However, the special symmetry position at the intersection of two mirror planes and a twofold axis *m*2*m* would allow only for a moment direction parallel to the *a* axis for both types of dysprosium atom. Since the experimentally found moment direction is along the *c* direction, a symmetry reduction to the monoclinic magnetic space group *Cm*, has to be assumed. The two dysprosium positions have moments which are oriented antiparallel. The magnetic mode describing the uniaxial arrangement is  $G_z(+ - + -)$ , the signs referring to the enumeration of the *C1m1* space group (International Tables). The moment values are  $9.4 \mu_B$  and  $-8.6 \mu_B$  for Dy(1) and Dy(2) respectively. These values are close to the free ion value ( $g\mu_B = 10 \mu_B$  for  $Dy^{3+}$ ). This moment arrangement is similar to that found in TbGe<sub>2</sub> [5].

Figure 6 displays the temperature dependence of the magnetic intensity (040), leading to an ordering temperature of 29 K, in good agreement with the value of 28 K reported by Sekizawa [1].

TABLE 4

Observed and calculated integrated neutron intensities of  $\text{DyGe}_{1.90}$  at 293 K. The observed intensities marked with an asterisk were also found by X-ray in ref. 1

<i>h</i>	<i>k</i>	<i>l</i>	<i>POS</i>	<i>INUC</i>	<i>IOBS</i>	<i>ESD</i>	<i>h</i>	<i>k</i>	<i>l</i>	<i>POS</i>	<i>INUC</i>	<i>IOBS</i>	<i>ESD</i>
0	2	0	6.64	28	985	206	0	16	1	60.86	850	1063	61
0	4	0	13.23	805	734	206	2	10	0	60.91	1428	1767	112
0	6	0	19.87	29	695	201	0	10	2	62.11	1382	1356	95
1	1	0	24.40	2057	2669*	185	0	18	0	62.15	120	116	5
0	0	1	24.81	154	206	62	1	7	2	62.33	5587	5710*	152
0	2	1	25.69	3028	1848*	170	2	8	1	63.03	15	91	20
1	3	0	26.16	7	7	1	1	15	1	63.21	81	548	123
0	8	0	26.57	2074	1899*	180	1	17	0	64.06	37	891	167
0	4	1	28.19	14	141	195	2	12	0	65.55	2139	2266	135
1	5	0	29.40	925	1404*	205	1	9	2	65.68	1449	1601	86
0	6	1	31.95	3579	4169*	212	0	12	2	66.70	2075	2151	59
0	10	0	33.37	2143	1648*	141	2	10	1	66.77	5432	5730	151
1	7	0	33.72	8291	7868*	185	0	18	1	67.96	28	919	179
1	1	1	35.04	127	196	186	1	11	2	69.75	2896	3431	151
1	3	1	36.33	4547	5153*	207	1	17	1	69.78	862	1012	45
0	8	1	36.64	16	228	95	0	20	0	69.98	26	31	7
1	5	1	38.80	36586	36129*	262	2	14	0	70.82	160	282	74
1	9	0	38.82	1820	1793	13	2	12	1	71.21	3688	3574	99
0	12	0	40.29	2648	3098*	202	1	19	0	71.39	4557	4371	114
0	10	1	41.99	6376	6868*	156	0	14	2	71.93	157	358	138
1	7	1	42.28	6127	6170*	155	2	0	2	73.54	9776	9344	209
1	11	0	44.49	2981	2988*	198	2	2	2	73.94	0	0	0
1	9	1	46.59	2	0	0	1	13	2	74.50	138	178	118
0	14	0	47.36	154	1485	123	2	4	2	75.11	132	259	58
0	12	1	47.86	3632	4610*	184	0	20	1	75.49	1677	1599	135
2	0	0	49.42	9705	9752*	212	2	14	1	76.30	5718	6582	155
2	2	0	49.91	0	2	4	2	16	0	76.70	985	1195	82
1	13	0	50.62	147	187	51	1	19	1	76.86	172	279	34
0	0	2	50.80	9224	10125*	191	2	6	2	77.05	1	2	0
0	2	2	51.28	0	0	0	3	1	0	77.71	374	420	50
2	4	0	51.38	120	168	26	0	16	2	77.78	969	988	120
1	11	1	51.57	368	301	133	0	22	0	78.21	15	44	24
0	4	2	52.72	114	29	172	3	3	0	78.48	15	222	103
2	6	0	53.75	4	97	75	1	21	0	79.18	0	3	2
0	14	1	54.16	4922	4261*	167	2	8	2	79.74	1668	1897	98
0	16	0	54.63	796	744*	127	1	15	2	79.90	6582	6706	141
0	6	2	55.05	3	41	70	3	5	0	80.01	149	140	4
2	0	1	56.04	60	40	114	0	0	3	80.04	15	14	0
2	2	1	56.49	1601	2438	128	0	2	3	80.42	535	597	132
2	8	0	56.95	1192	1311	33	0	4	3	81.56	8	104	66
1	1	2	57.10	1028	1070	20	2	16	1	82.05	1094	1377	113
1	13	1	57.13	971	1010	20	3	7	0	82.29	1896	2357	114
1	15	0	57.15	5662	5889*	123	3	1	1	83.04	59	80	12
2	4	1	57.83	16	32	10	2	10	2	83.16	1793	2389	365
1	3	2	57.99	21	29	7	2	18	0	83.20	218	289	45
0	8	2	58.20	1158	1060	168	0	6	3	83.46	882	1132	196
1	5	2	59.75	482	505	121	0	22	1	83.54	982	1249	229
2	6	1	60.03	2548	2203	134	0	0	0	0	0	0	0

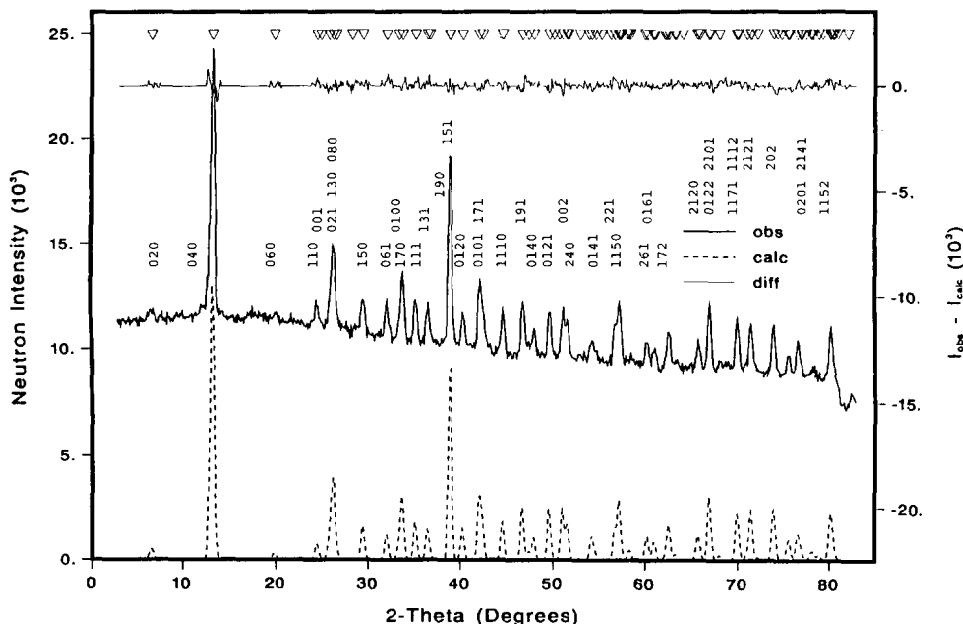
DyGe<sub>2</sub>, 4.2 K, 1.7078 Å

Fig. 4. Observed (solid line) and calculated (broken line) neutron diffraction pattern of DyGe<sub>2</sub> in the magnetic ordered state at 4.2 K.

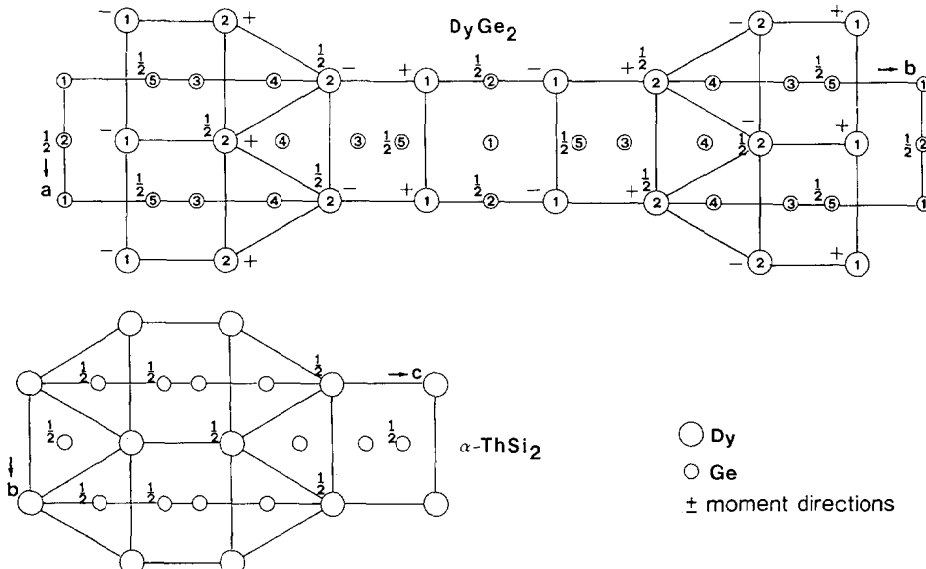


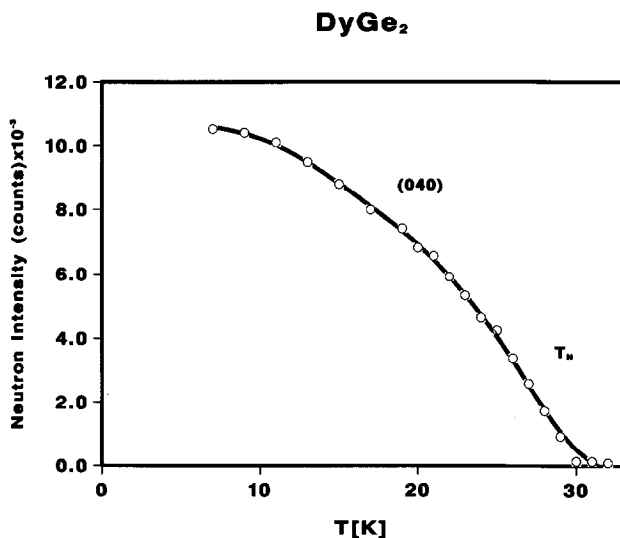
Fig. 5. Atomic and magnetic moment arrangements in the DyGe<sub>2</sub> type of structure when viewed along the [001] direction, showing its relation to the  $\alpha$ -ThSi<sub>2</sub> structure. The + - signs refer to the relative direction of the dysprosium moments.

TABLE 5

Interatomic distances for  $\text{DyGe}_{1.90}$  at 293 K up to 4.0 Å

<i>Atom's coordination number</i>	<i>Distance</i> (Å)	<i>Atom's coordination number</i>	<i>Distance</i> (Å)
Dy(1) 4Ge(5)	2.989(5)	4Ge(5)	3.736(15)
CN = 14 2Ge(2)	3.002(4)	2Ge(2)	3.987(1)
2Ge(1)	3.036(4)		
2Ge(3)	3.205(12)	Ge(3) 2Ge(4)	2.328(28)
2Dy(2)	3.955(7)	CN = 13 2Ge(5)	2.547(14)
2Dy(1)	3.987(1)	8Dy(2)	3.009(5)
		2Dy(1)	3.205(12)
Dy(2) 2Ge(4)	2.970(2)	2Ge(4)	3.756(23)
CN = 16 4Ge(3)	3.009(5)	2Ge(3)	3.987(1)
4Ge(4)	3.172(1)		
2Ge(5)	3.256(1)	Ge(4) 2Ge(4)	2.204(12)
2Dy(1)	3.955(7)	Ge(3)	2.328(28)
2Dy(2)	3.987(1)	2Dy(2)	2.970(18)
		4Dy(2)	3.172(10)
Ge(1) 4Ge(2)	2.8562(5)	2Ge(3)	3.756(23)
CN = 8 4Dy(1)	3.036(4)	2Ge(4)	3.987(10)
4Ge(5)	3.708(15)		
2Ge(1)	3.987(1)	Ge(5) 2Ge(3)	2.547(14)
		CN = 8 4Dy(1)	2.989(5)
Ge(2) 4Ge(1)	2.8562(5)	2Dy(2)	3.256(14)
CN = 8 4Dy(1)	3.002(4)		

Coordination polyhedra: (a)  $\text{Dy}^1\text{Dy}_4\text{Ge}_{10}$ , (b)  $\text{Dy}^2\text{Dy}_4\text{Ge}_{12}$ , (c)  $\text{Ge}^1\text{Dy}_4\text{Ge}_4$ , (d)  $\text{Ge}^2\text{Dy}_4\text{Ge}_4$ , (e)  $\text{Ge}^3\text{Dy}_{10}\text{Ge}_4$ , (f)  $\text{Ge}^4\text{Dy}_4\text{Ge}_3$ , (g)  $\text{Ge}^5\text{Dy}_6\text{Ge}_2$

Fig. 6. Temperature dependence of the neutron intensity of the (040) reflection of  $\text{DyGe}_2$ .

#### 4. Conclusions

The neutron diffraction measurements made in the course of the present investigation have shown that the compounds  $DyGe_{1.67}$  and  $DyGe_{1.9}$  are isotypic with compounds of similar composition found in the Tb-Ge system. The compound  $DyGe_{1.67}$  crystallizes in a defect  $\alpha$ -ThSi<sub>2</sub> type structure in which the germanium vacancies are highly ordered, leading to a superstructure with a unit cell six times larger than that of the basic tetragonal structure of the  $\alpha$ -ThSi<sub>2</sub> type. This superstructure can be considered as representing a stoichiometric compound with the chemical formula  $Dy_3Ge_5$ . The same kind of structure was found earlier for  $Y_3Ge_5$  [2, 11, 12]. For the compositions  $DyGe_{1.9}$  a new structure type, also related to the  $\alpha$ -ThSi<sub>2</sub> type, has been observed. This structure is isotypic with the structure of TbGe<sub>2</sub> described previously [5]. Neutron diffraction measurements made in the magnetically ordered regime have shown that  $DyGe_{1.9}$  has the same uniaxial antiferromagnetic structure as found for TbGe<sub>2</sub>. The magnetic structure of  $Dy_3Ge_5$  is antiferromagnetic also, but it is considerably more complex than that of  $DyGe_{1.9}$  and of the corresponding terbium compound. In this context it is of interest to study and compare the ordering of the  $DyGe_{1.62}$  composition of  $\alpha$ -ThSi<sub>2</sub> and compare its ordering with  $DyGe_{1.67}$ , which will be followed up in a future study.

#### Acknowledgments

The authors wish to thank Dr. P. Fisher and Dr. A. Furrer for fruitful discussions, and the Laboratorium für Neutronenstreuung of the ETH Zürich for technical support.

#### References

- 1 K. Sekizawa, *J. Phys. Soc. Jpn.*, **21** (1966) 1137, 274.
- 2 V. N. Eremenko, V. G. Batalin, I. Buyanov and I. M. Obushenko, *Dopov. Akad. Nauk. Ukr. RSR. Ser. B*, (6) (1977) 518.
- 3 P. Schobinger-Papamantellos and K. H. J. Buschow, *J. Less-Common Met.*, **144** (1989) 27.
- 4 P. Schobinger-Papamantellos and K. H. J. Buschow, *J. Magn. Magn. Mater.*, **82** (1989) 99.
- 5 P. Schobinger-Papamantellos, D. B. De Mooij and K. H. J. Buschow, *J. Less-Common Met.*, **144** (1988) 265.
- 6 H. M. Rietveld, *J. Appl. Crystallogr.*, **2** (1969) 65.
- 7 A. W. Hewat, *Harwell Rep. AERE-R7350*, 1973.
- 8 R. A. Young, E. Prince and R. A. Sparks, *J. Appl. Crystallogr.*, **15** (1982) 357.
- 9 V. F. Sears, in K. Skoeld and D. L. Price (eds.), *Methods of Experimental Physics*, Academic Press, New York, 1986, Vol. 23A, p. 521.
- 10 A. J. Freeman and J. P. Desclaux, *J. Magn. Magn. Mater.*, **12** (1979) 11.
- 11 F. A. Schmidt, O. D. McMasters and O. N. Carlson, *J. Less-Common Met.*, **26** (1972) 53.
- 12 V. A. Bruskov, O. I. Bodak, V. K. Pechaskii, E. I. Gladyshevskii and L. A. Muratova, *Sov. Phys.-Crystallogr.*, **28** (1983) 151.